Effect of G-Tract Length on the Topology and Stability of Intramolecular DNA Quadruplexes†

Phillip A. Rachwal,‡ Tom Brown,§ and Keith R. Fox*,‡

School of Biological Sciences, University of Southampton, Bassett Crescent East, Southampton SO16 7PX, U.K., and School of Chemistry, University of Southampton, Highfield, Southampton SO17 1BJ, U.K.

Received October 11, 2006; Revised Manuscript Received January 10, 2007

ABSTRACT: G-Rich sequences are known to form four-stranded structures that are based on stacks of G-quartets, and sequences with the potential to adopt these structures are common in eukaryotic genomes. However, there are few rules for predicting the relative stability of folded complexes that are adopted by sequences with different-length G-tracts or variable-length linkers between them. We have used thermal melting, circular dichroism, and gel electrophoresis to examine the topology and stability of intramolecular G-quadruplexes that are formed by sequences of the type $d(G_nT)_4$ and $d(G_nT_2)_4$ ($n = 3-7$) in the presence of varying concentrations of sodium and potassium. In the presence of potassium or sodium, $d(G_nT)_4$ sequences form intramolecular parallel complexes with the following order of stability: $n = 3 > n = 7 > n = 6 > n = 5 > n = 4$. $d(G_3T)_4$ is anomalously stable. In contrast, the stability of $d(G_nT_2)_4$ increases with the length of the G-tract ($n = 7 > n = 6 > n = 5 > n = 4 > n = 3$). The CD spectra for $d(G_nT)_4$ in the presence of potassium exhibit positive peaks around 260 nm, consistent with the formation of parallel topologies. These peaks are retained in sodium-containing buffers, but when $n = 4$, 5, or 6, CD maxima are observed around 290 nm, suggesting that these sequences [especially $d(G_5T)_4$] have some antiparallel characteristics. $d(G_3T_2)_4$ adopts a parallel conformation in the presence of both sodium and potassium, while all the other $d(G_nT_2)_4$ complexes exhibit predominantly antiparallel features. The properties of these complexes are also affected by the rate of annealing, and faster rates favor parallel complexes.

G-Rich sequences are known to fold into four-stranded structures that contain stacks of G-quartets (*1*−*4*). These structures can be formed by the association of four separate DNA strands (*5*), the dimerization of two strands that each contain two G-tracts (*6*), or the intramolecular folding of a single strand that contains four G-tracts (*7*−*10*). Quadruplex formation requires the presence of monovalent cations (*11*, *12*) (especially potassium), while stable folding is usually inhibited by lithium (*13*). The cations fit within the central core of guanine carbonyls and can lie between or within the plane of each quartet.

There is considerable interest in quadruplexes since G-rich sequences with the potential to adopt these structures are found in several biologically important DNA regions, such as gene promoters and telomeres (*6*, *14*). Telomeres consist of long repeats of G-rich sequences, $(GGGTTA)_n$ in humans and higher eukaryotes, $(G_4T_2)_n$ in *Tetrahymena*, and $(G_4T_4)_n$ in *Oxytricha*. A number of other nontelomeric G-rich DNA sequences may also form quadruplexes, and these have been identified in the NHE element of the *c-myc* promoter (*15*−*18*), the promoters of the Ki-*ras* (*19*), *bcl*2 (*20*, *21*), and *c-kit* oncogenes (*22*), the VEGF gene (*23*) and hypoxia inducible factor 1α (*24*), fragile X-syndrome (*25*), and other trinucleotide repeat sequences (*26*), the retinblastoma susceptibility gene (*27*), the chicken β-globin gene (*28*), and the insulin gene (*29*). There is also an overabundance of G-rich sequences in the regulatory regions of muscle-specific genes (*30*). Genome searches reveal that G-rich sequences with the potential to form quadruplexes are abundant in the human genome (*31*−*33*), the most common of which are successive G-tracts that are separated by single T or A residues. We have performed simple BLAST searches on repeated sequences of the type $d(G_nT)_4$ and find that these occur 147, 65, 120, and 2 times and once in the human genome when $n = 3-7$, respectively, and for $(G_nTT)_4$ for which there are 15, 75, and 6 occurrences when $n = 3-5$, respectively [we find no examples of $d(G_6TT)_4$ and $d(G_7TT)_4$].

Quadruplexes are known to adopt several different topologies, depending on their sequence and the ionic conditions. The four strands are all parallel in the intermolecular quadruplex (*5*), and the nucleotides are all in the *anti* conformation. However, multiple forms have been proposed for intramolecular quadruplexes in which the bases are both *syn* and *anti* (*1*). The strands can be arranged antiparallel to each other with the loops at the top and bottom of the stacked quartets (*1*, *9*) or in a parallel orientation with the loops in a lateral arrangement running between the bottom of one stack and the top of the other (*10*). Although there is still debate about which structure is biologically relevant (*34*), NMR (*35*), CD (*36*), and crystallographic studies (*10*) suggest that the human telomeric repeat $d(GGGTTA)_n$ adopts a

†P.A.R. is supported by a research studentship from BBSRC.

* To whom correspondence should be addressed: School of Biological Sciences, University of Southampton, Bassett Crescent East, Southampton SO16 7PX, U.K. Telephone: +44 23 8059 4374. Fax: +44 23 8059 4459. E-mail: k.r.fox@soton.ac.uk.

‡ School of Biological Sciences, University of Southampton, Bassett Crescent East.

§ School of Chemistry, University of Southampton, Highfield.

10.1021/bi062118j CCC: $37.00
Published on Web 02/21/2007

parallel structure in the presence of potassium. Several recent studies have shown that sequences closely related to the human telomeric repeat adopt a mixed topology with one double-chain reversal and two edgewise loops (*37*−*39*).

Some G-rich sequences form exceptionally stable complexes, such as the NHE element of *c-myc* and the inhibitor of HIV integrase $d(G_3T)_4$, which persist even in the presence of the complementary C-rich strand (*40*). However, there are few clear rules for predicting which G-rich sequences form the most stable quadruplexes or what topologies they will adopt. Quadruplex stability and topology are affected by the length of the loops between the G-tracts (*41*); G_3 tracts separated by short T-loops generate parallel topologies, while longer T-loops form antiparallel complexes (*41*). The stability is also affected by the sequence of the loops (*40*, *42*, *43*) and the bases that flank the quadruplex (*44*−*46*). However, there have been few studies on how formation is affected by the length of the G-stack. One might simply predict that longer G-stacks will increase quadruplex stability; however, for an intramolecular complex, this will affect the distance spanned by the connecting loops and may alter the folding pattern. Work with the thrombin-binding aptamer, which is based on two stacked quartets, has shown that the melting temperature is increased by ~20 °C upon addition of an extra G-quartet (*43*). In contrast, the *Tetrahymena* sequence $d(G_4T_2)_n$, which differs from the human sequence by exchanging A for G in each repeat, could in principle generate four stacked G-quartets linked by two-base loops. However, although this is observed for the intermolecular dimer (*47*), the intramolecular complex instead folds to form only three quartets with variable loops consisting of TGGT, TTG, and TT (*48*).

We have therefore explored how the length of the G-stack affects quadruplex stability and structure using synthetic oligonucleotides with $d(G_nT)_4$ and $d(G_nT_2)_4$ sequences ($n = 3-7$). The stability has been assessed by determining the melting temperatures under different ionic conditions, using a fluorescence melting assay as previously described (*40*, *42*, *49*), while structural changes are assessed from the CD spectra, since parallel and antiparallel quadruplexes generate characteristic CD spectra (*44*, *50*−*52*).

MATERIALS AND METHODS

Oligonucleotides. All oligonucleotides were synthesized on an Applied Biosystems ABI 394 automated DNA/RNA synthesizer on the 0.2 or 1 μmole scale. Phosphoramidite monomers and other reagents were purchased from Applied Biosystems or Link Technologies. The sequences of the oligonucleotides used in this work are given in Table 1. All oligonucleotides were prepared with 5′-fluorescein and 3′-dabcyl (fluorescein C6 phosphoramidite and dabcyl cpg purchased from Link Technologies Ltd.) for use in the fluorescence melting experiments, and the same sequences were used for the circular dichroism studies. The bases adjacent to the fluorophore and quencher were the same for all the oligonucleotides to prevent any differences in their effects on quadruplex formation and stability.

Gel Electrophoresis. Nondenaturing gel electrophoresis was performed using 16% polyacrylamide gels, which were run in TBE buffer that had been supplemented with 50 mM NaCl or KCl. Bands in the gels were visualized under UV light. The oligonucleotide concentration was 20 μM, and the samples were slowly annealed in the appropriate buffer. Denaturing electrophoresis was performed using 14% polyacrylamide gels containing 8 M urea.

Table 1: Sequences of Oligonucleotides Used in This Work

oligonucleotide sequence[a]	name
G_nT series	
5′-F-TGGGTGGGTGGGTGGGT-Q	G_3T
5′-F-TGGGGTGGGGTGGGGTGGGGT-Q	G_4T
5′-F-TGGGGGTGGGGGTGGGGGTGGGGGT-Q	G_5T
5′-F-TGGGGGGTGGGGGGTGGGGGGTGGGGGGT-Q	G_6T
5′-F-TGGGGGGGTGGGGGGGTGGGGGGGTGGGGGGGT-Q	G_7T
G_nT_2 series	
5′-F-TGGGTTGGGTTGGGTTGGGT-Q	G_3T_2
5′-F-TGGGGTTGGGGTTGGGGTTGGGGT-Q	G_4T_2
5′-F-TGGGGGTTGGGGGTTGGGGGTTGGGGGT-Q	G_5T_2
5′-F-TGGGGGGTTGGGGGGTTGGGGGGTTGGGGGGT-Q	G_6T_2
5′-F-TGGGGGGGTTGGGGGGGTTGGGGGGGTTGGGGGGGT-Q	G_7T_2

[a] F represents fluorescein and Q dabcyl.

Circular Dichroism. CD spectra were recorded on a Jasco J-720 spectropolarimeter as previously described (*42*). Oligonucleotide solutions (5 μM) were prepared in 10 mM lithium phosphate (pH 7.4) containing either 50 mM potassium chloride or 50 mM sodium chloride. The samples were heated to 95 °C and annealed by being slowly cooled to 15 °C over a period of 12 h. Spectra were recorded between 220 and 320 nm in 5 mm path length cuvettes. Spectra were averaged over 16 scans, which were recorded at 100 nm/min with a response time of 1 s and a bandwidth of 1 nm. A buffer baseline was subtracted from each spectrum, and the spectra were normalized to have zero ellipticity at 320 nm.

Fluorescence Melting. Fluorescence melting curves were determined in a Roche LightCycler as previously described (*40*, *42*, *49*) in a total reaction volume of 20 μL. Oligonucleotides (final concentration of 0.25 μM) were prepared in 10 mM lithium phosphate (pH 7.4), which was supplemented with various concentrations of potassium or sodium chloride. The LightCycler has one excitation source (488 nm), and the changes in fluorescence were measured at 520 nm. For several of the oligonucleotides, initial experiments revealed that there was considerable hysteresis between the heating and annealing profiles when the temperature was changed at a rate of 0.2 °C/s, indicating that the process was not at thermodynamic equilibrium. Melting experiments were therefore performed at a much slower rate of heating and cooling (0.1 °C/min) by changing the temperature in 1 °C steps, leaving the samples to equilibrate for 10 min at each temperature before the fluorescence was recorded. Under these conditions, no hysteresis was observed (except for some experiments with G_7T_2). In a typical experiment, the oligonucleotides were first denatured by heating to 95 °C for 5 min. They were then annealed by cooling to 30 °C at a rate of 0.1 °C/min and melted by heating to 95 °C at the same rate. The fluorescence was recorded during both the annealing and melting steps. In some instances, the formation of intramolecular or intermolecular complexes was examined by determining the melting curves using a range of oligonucleotide concentrations (from 20 nM to 2 μM).

Data Analysis. T_m values were obtained from the maxima of the first derivatives of the melting profiles using the LightCycler software or, together with ΔH, from van't Hoff

analysis of the melting profiles. In some instances, the melting curves showed a linear change in fluorescence with temperature in regions outside the melting transition. We accounted for this by fitting a straight line to the first and last portions of the fluorescence curve. The fraction folded was calculated as previously described (*53*) from the difference between the measured fluorescence and the upper and lower baselines. All reactions were performed at least twice, and the calculated T_m values usually differed by <0.5 °C with a 5% variation in ΔH. Since $\Delta G = 0$ at the T_m, ΔS was estimated to be $\Delta H/T_m$. Values for ΔG at 310 K were then estimated from $\Delta G = \Delta H - T\Delta S$ (assuming that $\Delta C_p = 0$). This analysis assumes a simple two-state equilibrium between the folded and unfolded forms. The presence of polymorphic quadruplex structures will lead to shallower melting profiles and therefore smaller apparent values for ΔH. The number of specifically bound monovalent cations (Δn) was calculated from the slopes of plots of ΔG against $\log[M^+]$ as previously described (*54*, *55*).

RESULTS

We have recorded the CD spectra and thermal melting profiles of two series of oligonucleotides that contain G-tracts of varying lengths. Oligonucleotides in the first series contain four identical G-tracts with lengths between three and seven bases, which are separated by single thymines. In the second series, the G-tracts are each separated by two thymines. Both series of oligonucleotides were prepared for use in fluorescence melting experiments and contain fluorescein at the 5′-end and dabcyl at the 3′-end. Previous studies have shown that the addition of fluorescent groups has only small effects on quadruplex stability (*56*).

Circular Dichroism

Several studies have shown that the CD spectra of quadruplexes can be used to indicate whether they fold in a parallel or antiparallel configuration (*44*, *50*−*52*). Antiparallel quadruplexes exhibit a positive CD signal at around 295 nm, with a negative signal or shoulder around 260 nm. In contrast, parallel quadruplexes display a positive signal around 260 nm, with a negative peak at 240 nm. Unfolded oligonucleotides do not display these spectral signatures. Clearly, these signals not only reflect the arrangements of the strands but also are sensitive to the *syn*/*anti* orientations around the glycosidic bonds. Parallel topologies have all-*anti* glycosidic angles, while antiparallel ones have *syn* and *anti* in varying ratios depending on the particular arrangement. Nonetheless, they are a good indicator of changes in the global quadruplex configuration.

d(G$_n$T)$_4$. The CD spectra of oligonucleotides with a d(G$_n$T)$_4$ sequence ($n = 3-7$) in the presence of potassium or sodium are presented in Figure 1. These were obtained after slowly cooling the oligonucleotides from 95 °C, though identical spectra were observed when the complexes were rapidly cooled. It can be seen that, in the presence of potassium, all the sequences display a major positive peak around 260 nm with a minimum around 240 nm, which is typical of a parallel arrangement of the strands. G$_3$T and G$_4$T exhibit no ellipicity around 290 nm, though the other sequences show some signal in this region which is greatest for G$_6$T. This second peak suggests that these sequences may

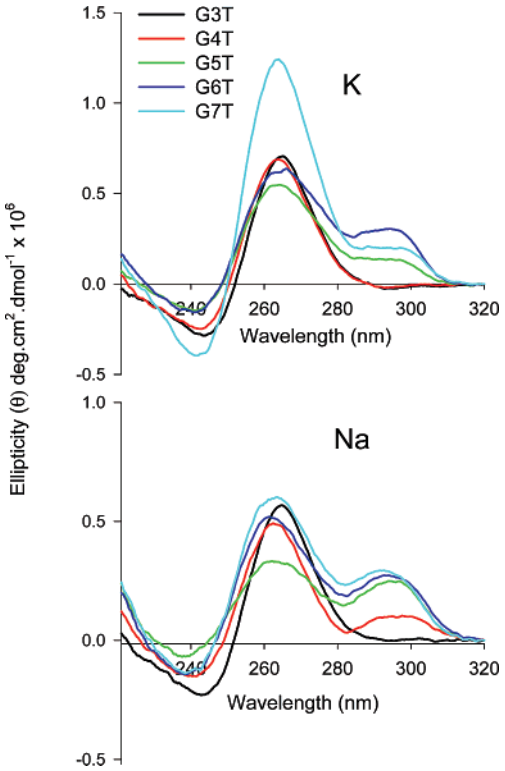

FIGURE 1: CD spectra of the fluorescently labeled oligonucleotides of the series d(G$_n$T)$_4$. The oligonucleotides (5 μM) were dissolved in 10 mM lithium phosphate (pH 7.4) containing 50 mM potassium chloride (top traces) or 50 mM sodium chloride (bottom traces): black for G$_3$T, red for G$_4$T, green for G$_5$T, blue for G$_6$T, and cyan for G$_7$T.

exhibit structural polymorphism with a significant fraction adopting an antiparallel configuration (though it is possible that unpaired guanines in the loops might also affect the CD spectra). However, these spectra are also typical of mixed parallel/antiparallel topologies (*18*, *20*). In the presence of sodium, G$_3$T again shows a single peak at 260 nm, indicative of a parallel complex, while the other oligonucleotides display significant ellipticity at 295 nm. In sodium, the relative intensity of the 295 nm peak compared to that at 260 nm is greatest for G$_5$T.

These results confirm that the oligonucleotides all fold to form G-quadruplexes but suggest that their structures may be polymorphic. They predominantly fold into a parallel configuration (especially G$_3$T), though these coexist with significant amounts of the antiparallel form (especially G$_5$T in the presence of sodium). Via a comparison of these results with those published for sequences of the type (G$_3$T$_n$)$_4$ (*41*), it is clear that adding G bases to the sequence has an effect different from the effect of adding extra T bases to the loops. d(G$_3$T$_3$)$_4$ and d(G$_5$T)$_4$ have the same repeat length; however, the former adopts an antiparallel topology, while the latter is largely parallel.

d(G$_n$T$_2$)$_4$. The CD spectra of sequences containing four repeats of G$_n$T$_2$ ($n = 3-7$) in the presence of sodium or potassium are shown in Figure 2. In the presence of potassium, the spectra are different when the complexes are rapidly cooled on ice (inset) or slowly annealed. After the rapid cooling, the spectra are similar to those of the G$_n$T series, with a strong peak at 260 nm and a weaker one at 295 nm, indicating that the parallel configuration is the major form. In contrast, the peaks at 295 nm are much more

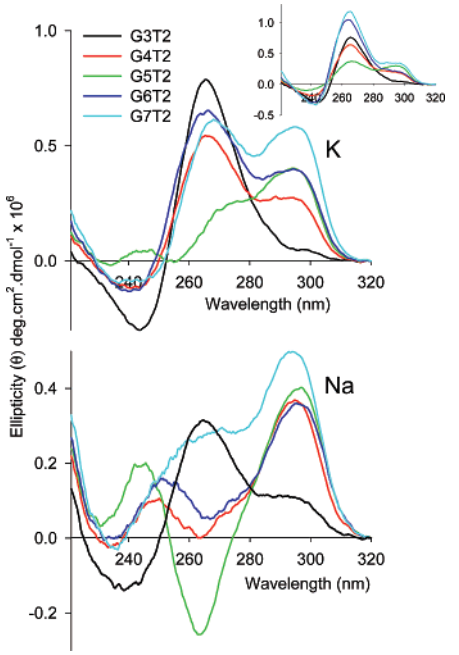

FIGURE 2: CD spectra of the fluorescently labeled oligonucleotides of the series $d(G_nT_2)_4$. The oligonucleotides (5 μM) were dissolved in 10 mM lithium phosphate (pH 7.4) containing 50 mM potassium chloride (top traces) or 50 mM sodium chloride (bottom traces): black for G_3T_2, red for G_4T_2, green for G_5T_2, blue for G_6T_2, and cyan for G_7T_2.

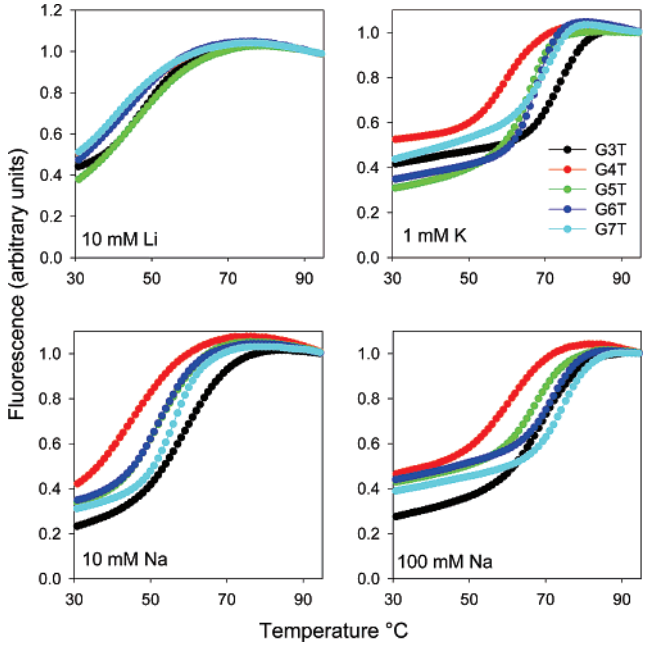

FIGURE 3: Fluorescence melting curves for oligonucleotides of the series $d(G_nT)_4$. The melting profiles were determined in 10 mM lithium phosphate (pH 7.4) containing different concentrations of potassium or sodium chloride as indicated. The curves have been normalized to the same final fluorescence value: black for G_3T, red for G_4T, green for G_5T, blue for G_6T, and cyan for G_7T.

pronounced when the oligonucleotides are slowly annealed. G_3T_2 appears to be mainly parallel, while G_4T_2 has a significant shoulder at 295 nm. G_5T_2 is predominantly in the antiparallel form, though the proportion of the antiparallel species appears to decrease with G_6T_2 and G_7T_2.

In the presence of sodium, the spectra exhibit large peaks at 295 nm, indicative of antiparallel complex formation. Even the shortest sequence, G_3T_2, reveals a significant shoulder in this region, though it is predominantly in the parallel form. In contrast, G_4T_2, G_5T_2, and G_6T_2 are mainly in an antiparallel form with no positive peak at 260 nm. G_7T_2 is mainly antiparallel but has a significant shoulder around 260 nm. These spectra in the presence of sodium are independent of the rate of cooling.

For these CD studies, we were concerned that the fluorophore and quencher might affect the conformational equilibrium. We therefore determined the CD spectra of unlabeled sequences that showed examples of very different spectra (G_3T, G_5T, and G_5T_2). These are shown in Figure 1 of Supporting Information and reveal only subtle changes in the details of the spectra. The positions and relative intensities of the peaks at 260 and 295 nm are largely unaffected by removal of the fluorescent groups.

Fluorescence Melting

$d(G_nT)_4$. Typical fluorescence melting curves for these oligonucleotides are shown in Figure 3, and the T_m and ΔH values determined at different ionic concentrations are summarized in Table 2. These labeled oligonucleotides are designed so that the fluorescence is quenched upon formation of the quadruplex, as the fluorophore (fluorescein) and quencher (dabcyl) are close together. These groups are separated when the complex melts, and there is a large increase in fluorescence. This cannot be used to distinguish

Table 2: Melting Temperatures and ΔH Values Derived from Fluorescence Melting Curves for Oligonucleotides of the Type $(G_nT)_4$ ($n = 3-7$)[a]

	T_m (°C)					ΔH (kJ/mol)				
	$n = 3$	$n = 4$	$n = 5$	$n = 6$	$n = 7$	$n = 3$	$n = 4$	$n = 5$	$n = 6$	$n = 7$
10 mM Li	48.3	41.8	43.7	43.4	43.1	122	102	104	111	100
0.1 mM K^+	58.4	46.1	50.0	51.8	54.3	210	119	175	227	236
1 mM K^+	73.8	58.6	65.5	67.6	71.3	291	200	272	322	326
5 mM K^+	85.4	71.3	76.4	79.1	86.5	299	273	324	391	381
10 mM K^+		76.0	80.8	83.3	88.4		291	282	374	351
1 mM Na^+	52.7	44.3	46.5	47.2	47.4	141	110	117	120	118
10 mM Na^+	59.8	46.5	52.3	52.3	54.0	177	118	179	177	213
50 mM Na^+	66.0	55.5	62.8	65.4	68.7	197	164	221	253	291
100 mM Na^+	69.7	60.8	67.7	71.9	75.1	246	186	239	294	314
200 mM Na^+	75.3	68.1	75.6	81.4	82.6	198	202	214	340	346

[a] The values were determined in 10 mM lithium phosphate (pH 7.4) containing different concentrations of sodium or potassium. Each value is the average of four determinations (two melting and two annealing profiles). T_m values are accurate to within 0.5 °C, while ΔH values varied by ~5%.

between the different folded forms, as the fluorophore and quencher are close together in both the parallel and the antiparallel topologies. All the sequences exhibit fluorescence changes that are consistent with quadruplex formation, and they are all much more stable in the presence of potassium than sodium. We confirmed that these transitions are not intermolecular complexes by examining the concentration dependence of the melting profiles (from 20 nM to 2 μM). These results (shown in Figure 2 of the Supporting Information) show that the T_m values are independent of concentration. We can therefore assume that these are intramolecular complexes over this range of concentrations. All these melting curves were fully reversible at this rate of heating and cooling (0.1 °C/min).

The first panel of Figure 3 shows the transitions in the presence of 10 mM lithium alone. Surprisingly, these complexes display a melting profile (with a T_m of ~45 °C), even in the absence of potassium or sodium. This is similar to the effect seen with sequences containing four G_3 tracts that are connected by non-nucleosidic linkers (*42*). Although this may indicate some quadruplex formation, it may be significant that these complexes all have very similar T_m and ΔH values, in contrast to their behavior in the presence of sodium or potassium. The addition of even low concentrations of potassium causes a dramatic increase in stability, and the complexes are too stable to measure at potassium concentrations of >10 mM.

In the presence of ≤1 mM potassium, G_3T is the most stable while G_4T is the least stable. In general, the stability increases with the length of the G-tract ($n = 4 < n = 5 < n = 6 < n = 7$), though the behavior of G_3T is anomalous since it is more stable than G_7T. All the complexes become more stable when the potassium ion concentration increases. ΔH values for these transitions were estimated from van't Hoff analysis of the melting profiles, assuming a two-state equilibrium, and these are also summarized in Table 2. The presence of polymorphic quadruplex structures will lead to shallower melting profiles and therefore smaller apparent values of ΔH. This may explain why there is no simple correlation between ΔH and the number of G bases in each G-tract, though in general the values are higher for the longer G-tracts (with the exception of G_3T).

The results of similar experiments in the presence of 10 and 100 mM sodium are shown in the bottom panels of Figure 3, and all the data are summarized in Table 2. In contrast to potassium, the addition of 1 mM sodium has an only small effect on the melting profiles, increasing the T_m values by only 3−4 °C relative to that in 10 mM lithium. In the presence of 10 mM sodium, G_3T again forms the most stable structure; G_4T is the least stable, and G_5T, G_6T, and G_7T have similar T_m values. G_7T becomes the most stable when the sodium concentration is increased to 100 mM, though G_3T is still more stable than G_4T, G_5T, or G_6T. In general, the ΔH values are higher for the longer G-tracts, though G_3T is again anomalous.

$d(G_nT_2)_4$. The results of similar studies with oligonucleotides in which the G-tracts are separated by two T bases are shown in Figure 4, and the T_m and ΔH values are summarized in Table 3. No melting transitions were observed in the presence of lithium alone. In the presence of either potassium or sodium, the least stable complex is formed by G_3T_2, while G_7T_2 is the most stable. In potassium, the order

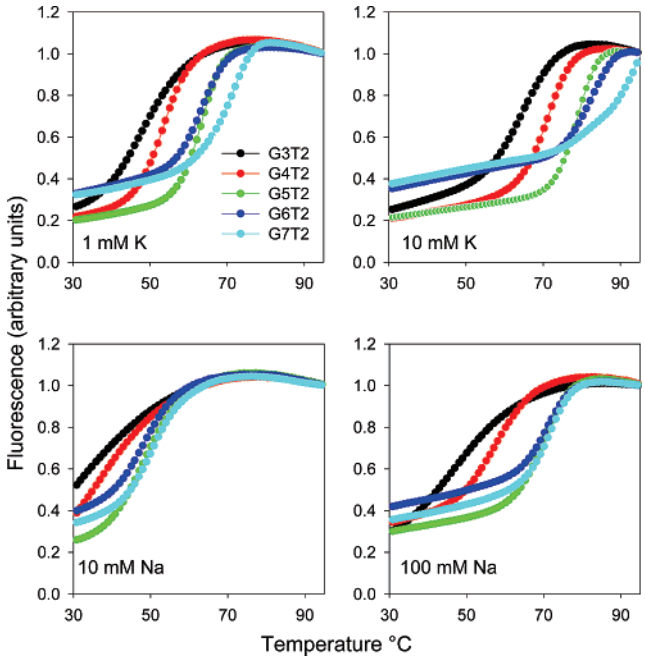

FIGURE 4: Fluorescence melting curves for oligonucleotides of the series $d(G_nT_2)_4$. The melting profiles were determined in 10 mM lithium phosphate (pH 7.4) containing different concentrations of potassium or sodium chloride as indicated. The curves have been normalized to the same final fluorescence value: black for G_3T, red for G_4T, green for G_5T, blue for G_6T, and cyan for G_7T.

of stability is as follows: $G_3T_2 < G_4T_2 < G_5T_2 = G_6T_2 < G_7T_2$ (though there is some hysteresis with G_7T_2 for which the melting temperatures are 3, 8, and 10 °C higher than the annealing temperatures in the presence of 0.1, 1, and 5 mM potassium, respectively). These structures are unstable in the presence of sodium concentrations below 10 mM, and the order of stability is as follows: $G_3T_2 < G_4T_2 < G_5T_2 = G_6T_2 = G_7T_2$.

Ionic Strength Dependence

The ΔH values for these transitions exhibit a strong dependence on the ionic strength, which is consistent with the presence of specific ion binding sites within the quadruplex (*54*). The slopes of plots of ΔG versus $\log[M^+]$ can be used to determine the stoichiometry of ion binding as previously described (*54*, *55*), yielding values of Δn (the difference between the number of ions bound in the folded and unfolded states). Figure 5 shows the variation in Δn with the number of guanines in each stack for both series of oligonucleotides, in the presence of sodium or potassium. We have previously determined a value of 2.6 for the human telomeric repeat sequence in the presence of potassium (*42*), and a value of 3.7 ± 0.2 has been reported for T30695, which has the same repeat sequence as G3T (*54*). For a structure containing three stacked G-quartets, we would predict that Δn should be either 2 (the number of potassium ions located between the stacked quartets) or 4 (including two further ions that may be coordinated between the loops and the terminal quartets). A value of 2 seems more likely for a parallel topology, in which the loops do not interact with the terminal quartets. In either case, we would expect that adding a further G-quartet should increase the value of Δn

Table 3: Melting Temperatures and ΔH Values Derived from Fluorescence Melting Curves for Oligonucleotides of the Type $(G_nT_2)_4$ ($n = 3-7$)[a]

	T_m (°C)					ΔH (kJ/mol)				
	$n = 3$	$n = 4$	$n = 5$	$n = 6$	$n = 7$	$n = 3$	$n = 4$	$n = 5$	$n = 6$	$n = 7$
0.1 mM K^+		36.3	47.0	46.7	51.1[b]		99	188	186	213[b]
1 mM K^+	48.1	53.3	62.9	63.0	68.3[b]	136	224	294	283	289[b]
5 mM K^+	60.1	66.1	74.1	74.7	81.9[b]	199	263	359	345	322[b]
10 mM K^+	65.0	71.4	78.9	80.1		241	286	376	371	
50 mM K^+	76.2	82.4	89.7			267	308	336		
1 mM Na^+				42.5	41.4				100	101
5 mM Na^+			45.1	47.2	47.1			134	123	132
10 mM Na^+		37.3	46.5	52.3	50.7		97	157	155	168
50 mM Na^+	40.3	49.9	62.3	65.4	63.7	99	152	248	260	278
100 mM Na^+	46.8	57.7	70.2	71.9	71.9	113	188	290	314	318
200 mM Na^+	54.4	66.2	78.3	81.4	81.3	144	225	323	354	334

[a] The values were determined in 10 mM lithium phosphate (pH 7.4) containing different concentrations of sodium or potassium. Each value is the average of four determinations (two melting and two annealing profiles). T_m values are accurate to within 0.5 °C, while ΔH values varied by ~5%. [b] Hysteresis was observed between the melting and annealing profiles.

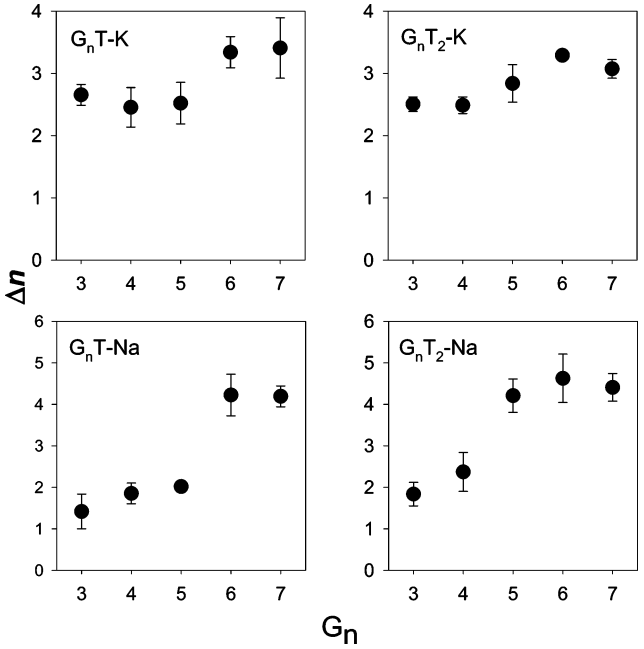

FIGURE 5: Variation in the number of potassium or sodium ions specifically bound to each quadruplex (Δn, *y*-axis) as a function of the length of the G-tracts (G_n, *x*-axis). The values for Δn were determined from the dependence of ΔG on ionic strength, as described in the text.

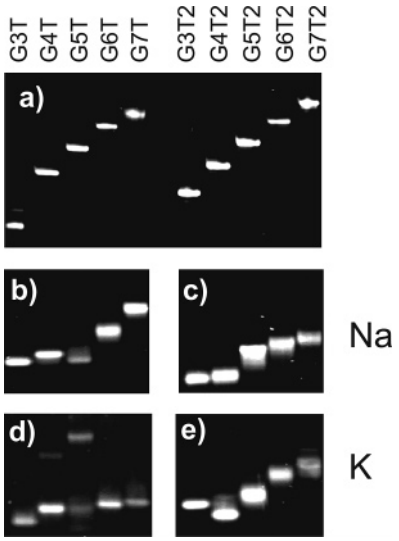

FIGURE 6: Mobility of the fluorescently labeled oligonucleotides in polyacrylamide gels: (a) mobility on a 14% polyacrylamide gel containing 8 M urea and (b–e) mobility on 16% nondenaturing polyacrylamide gels supplemented with 50 mM NaCl (b and c) or 50 mM KCl (d and e).

by 1. It is therefore significant that, for the G_nT series in the presence of potassium, Δn is the same for G_3T, G_4T, and G_5T, suggesting that these each contain only three stacked G-quartets. Δn increases by ~1 for G_6T and G_7T, suggesting that these complexes contain an additional quartet. The values of Δn exhibit even less variation for the G_nT_2 series in the presence of potassium, again suggesting that there are only three stacked G-quartets. The variations in Δn are more pronounced in the presence of sodium; G_3T, G_4T, and G_5T have similar values, between 1.5 and 2, which rises to ~4 for G_6T and G_7T. A similar pattern is seen for the G_nT_2 series in sodium, though the transition between Δn values of 2 and 4 occurs with G_5T_2. These results are considered further in the Discussion.

Gel Mobility

We sought to further explore the topologies of these intramolecular quadruplexes by comparing their mobilities in polyacrylamide gels, and the results are presented in Figure 6. As expected, the unfolded oligonucleotides run as single bands on denaturing polyacrylamide gels (Figure 6a), with mobilities that depend on their length. G_3T appears to have an anomalously fast mobility, probably because it is still partially folded even under these harsh conditions. In contrast, the relative mobility of the various folded species is very different. In the presence of sodium (Figure 6b,c), although single bands are observed for each oligonucleotide, G_3T, G_4T, and G_5T have similar mobilities, while G_6T and G_7T run more slowly (Figure 6b). The pattern is different for the G_nT_2 series (Figure 6c) in which G_3T_2 and G_4T_2 have similar mobilities, while G_5T_2, G_6T_2, and G_7T_2 run more slowly and have similar mobilities. These patterns are similar to the variations in the apparent number of sodium ions released on the melting of each complex (Figure 5, bottom panels), suggesting that they reflect the number of stacked G-quartets in each complex.

The gel mobilities in the presence of 50 mM potassium show a different pattern. For the G_nT series, two bands are evident with G_3T, G_4T, and G_5T, the faster of which

comigrates with G_6T and G_7T, though G_3T has a slightly faster mobility. The intensity of the slowly migrating species was dependent on the method of annealing, and these were more abundant when the complexes were prepared by slow annealing (as shown). We assume that the slow-migrating species (which is especially abundant with G_5T) corresponds to intermolecular complexes, while the faster species are intramolecular. It should be noted that these complexes were prepared with 20 μM oligonucleotide (in contrast to 0.25 μM oligonucleotide required for the fluorescence melting experiments), and this 80-fold higher concentration will favor the formation of bimolecular or tetramolecular complexes. The observation that all the faster species have similar mobilities is consistent with the suggestion that they contain the same number of stacked G-quartets. For the G_nT_2 series, the mobility decreases as the number of G bases increases from G_4T_2 to G_7T_2, though G_3T_2 is unusually slow.

DISCUSSION

These results demonstrate that, as expected, all the G-rich sequences fold to form quadruplexes; the CD spectra exhibit positive peaks at either 260 or 295 nm, and the fluorescence melting profiles show a folded conformation in which the fluorophore and quencher are close together at low temperatures. The folded complexes are stabilized by addition of monovalent cations, and potassium consistently generates more stable complexes than sodium. The complexes appear to be intramolecular (rather than intermolecular) as the T_m values are generally independent of oligonucleotide concentration.

These results address three main questions concerning these quadruplexes: what their relative stabilities are, how many stacked G-quartets are present in each complex (i.e., are any of the G bases placed in the loops), and whether they adopt a parallel or antiparallel topology.

Stabilities. Although the fluorescence melting data cannot distinguish between different conformations, they provide an estimation of the overall stability of the different complexes. Under all the conditions that were investigated, the stability increases with the length of the G-tracts, except for G_3T, which has an anomalously high stability in the presence of both sodium and potassium. In low concentrations of both potassium and sodium, the order of T_m values is as follows: $G_3T > G_7T > G_6T > G_5T > G_4T$. The unusual stability of G_3T has previously been noted (*40*, *41*) and may result from conformational changes after the initial formation of the complex (*54*). This order is retained at higher potassium concentrations, except that G_7T and G_3T display very similar T_m values. In high concentrations of sodium, G_3T is further down the rank order of stabilities and is intermediate between G_5T and G_6T. The rank order of stability for the second series, in which the G-tracts are separated by two T bases, shows that longer G-tracts produce more stable structures. In the presence of potassium, G_5T_2 and G_6T_2 have very similar T_m values, while G_7T_2, G_6T_2, and G_5T_2 are similar in the presence of sodium. These results demonstrate that there is no simple relationship between quadruplex stability and the length of the G-tracts, though the behaviors in sodium and potassium are similar.

Parallel or Antiparallel. The presence of peaks at 260 or 295 nm in the CD spectrum is typically used as an indicator of whether the quadruplex adopts a parallel or antiparallel topology (*44*, *50*−*52*), as a result of the *syn*/*anti* configuration of the glycosidic bonds, which are *anti* for the parallel structures and *syn* and *anti* in varying ratios for antiparallel complexes (*60*, *61*). The results show that the shortest oligonucleotides (G_3T, G_3T_2, and G_4T) adopt parallel topologies in the presence of both sodium and potassium. This is consistent with previous studies on the effect of loop length (*41*), which suggested that short loops are not sufficient to generate antiparallel topologies. The parallel structure proposed for G_3T (T30695, HIV integrase inhibitor) is at variance with the published NMR structure, which suggested an antiparallel structure containing two stacked G-quartets (*54*, *57*, *59*), though it has been noted that this structure requires further investigation (*59*).

In the presence of potassium, the oligonucleotides with single T residues between the G-tracts all adopt a structure for which the CD signature suggests a predominantly parallel topology. The parallel topology also appears to be the main form in the presence of sodium, though the greater CD signal at 295 nm suggests that this may be in equilibrium with the antiparallel form. This is especially noticeable for G_5T, for which the peaks at 260 and 295 nm are closer in intensity. In contrast, the CD spectra of G_6T are very similar in the presence of both sodium and potassium.

The sequences with two T bases between the G-tracts show a much stronger propensity to adopt the antiparallel conformation (except G_3T_2, for which the potassium and sodium forms are exclusively parallel). G_4T_2 is largely parallel in the presence of potassium but switches to the antiparallel form in sodium. G_5T_2 adopts a topology which is mainly antiparallel in both sodium and potassium. In contrast, G_6T_2 and G_7T_2 show mixed conformations in potassium but switch to mainly antiparallel conformations in sodium. The strong signal at 295 nm for G_6T and G_7T argues against aggregation into an intermolecular form, which would be expected to be parallel.

How Many G-Quartets? For the longer sequences, it is clear that a folded structure must contain some G residues in the loops as, for instance, a single T will be insufficient to span between the top and bottom of a stack of seven potential G-quartets in G_7T. The values of Δn, derived from the thermodynamic parameters, should be interpreted with caution, as there may be multiple forms in equilibrium, which may vary according to the ionic strength. However, they do indicate some trends concerning the number of stacked G-quartets in each complex, which are consistent with the gel mobility patterns. In potassium, G_3T, G_4T, and G_5T all appear to contain only three stacked quartets, suggesting that their loops contain a single T, GT, and GGT, respectively. For G_4T and G_5T, several structures could be envisaged depending on which G bases are stacked and which are in the loops; several different forms may coexist in solution in which the G-strands slip relative to each other. The values of Δn for G_6T and G_7T appear to increase by one, suggesting that these may contain four stacked G-quartets, with GGT and GGGT in their (lateral) loops. A similar transition is evident for G_nT between $n = 5$ and 6 in the presence of sodium, though in this case the value of Δn is only $\sim$2 for G_3T, G_4T, and G_5T and increases to 4 for G_6T and G_7T. The lower value might indicate the presence of one fewer stacked quartet or more likely indicates that the sodium ions

are less tightly held between the terminal G bases and the loops.

In the presence of potassium, the values of Δn are similar for all the complexes. The similarity in G_3T_2 and G_4T_2 is consistent with the NMR structure of the intramolecular *Tetrahymena* repeat (G_4T_2) which shows an antiparallel complex containing three stacked G-quartets. In this case, it appears that increasing the length of the G-tracts does not increase the number of stacked G-quartets and the additional G bases must reside in the loops. In sodium, G_3T_2 and G_4T_2 have the same number of G-quartets, which increase for G_5T_2, G_6T_2, and G_7T_2.

Comparison with Other Studies. In our previous publication (*40*), we suggested that G_3T_2 was more stable than G_4T_2, in contrast to our study in which the melting temperatures increase with the longer G-tracts. Several factors may contribute to this difference. First, this study was performed in 10 mM lithium phosphate buffer to which different concentrations of potassium or sodium had been added, in contrast to the earlier work which simply used sodium or potassium phosphate buffers. Second, different fluorophores and quenchers have been used in the two studies, which may affect the relative stabilities. In this study, these are separated from the quadruplex by single thymines at each end, while in the previous work, the fluorophores were positioned immediately adjacent to the terminal G bases. Third, and probably most importantly, we have employed much slower rates of heating and cooling. Risitano and Fox (*40*) measured annealing profiles at a rate of temperature change of 0.1 °C/s and noted that there was hysteresis between the heating and cooling curves, some of which were biphasic. In this study, we have shown that, in the presence of potassium, the CD spectra of the G_nT_2 series are affected by the rate of annealing; rapid cooling produces parallel structures, while slow cooling generates antiparallel complexes. In this study, we therefore used a 60-fold slower rate of temperature change in determining the melting profiles (0.1 °C/min) and observed no hysteresis between the heating and cooling curves, and the profiles were all monophasic. This work has therefore been performed under equilibrium conditions, allowing a proper analysis of relative stabilities for the different folded quadruplexes.

SUPPORTING INFORMATION AVAILABLE

Full details comparing the CD spectra of labeled and unlabeled oligonucleotides and the concentration dependence of the melting profiles. This material is available free of charge via the Internet at http://pubs.acs.org.

REFERENCES

1. Simonsson, T. (2001) G-Quadruplex DNA structures: Variations on a theme, *Biol. Chem. 382*, 621−628.
2. Burge, S., Parkinson, G. N., Hazel, P., Todd, A. K., and Neidle, S. (2006) Quadruplex DNA: Sequence, topology and structure, *Nucleic Acids Res. 34*, 5402−5415.
3. Keniry, M. A. (2000) Quadruplex structures in nucleic acids, *Biopolymers 56*, 123−146.
4. Davies, J. T. (2004) G-Quartets 40 years later: From 5′-GMP to molecular biology and supramolecular chemistry, *Angew. Chem., Int. Ed. 43*, 668−698.
5. Phillips, K., Dauter, Z., Murchie, A. I., Lilley, D. M. J., and Luisi, B. (1997) The crystal structure of a parallel-stranded guanine tetraplex at 0.95 Angstrom resolution, *J. Mol. Biol. 273*, 171−182.
6. Sundquist, W. I., and Klug, A. (1989) Telomeric DNA dimerizes by formation of guanine tetrads between hairpin loops, *Nature 342*, 825−829.
7. Henderson, E., Hardin, C. C., Walk, S. K., Tinoco, I., and Blackburn, E. H. (1987) Telomeric DNA oligonucleotides form novel intramolecular structures containing guanine-guanine base pairs, *Cell 51*, 899−908.
8. Macaya, R. F., Schultze, P., Smith, F. W., Roe, J. A., and Feigon, J. (1993) Thrombin-binding DNA aptamer forms a unimolecular quadruplex structure in solution, *Proc. Natl. Acad. Sci. U.S.A. 90*, 3745−3749.
9. Wang, Y., and Patel, D. J. (1993) Solution structure of the human telomeric repeat d[$AG_3(T_2AG_3)_3$] G-tetraplex, *Structure 1*, 76−94.
10. Parkinson, G. N., Lee, M. P. H., and Neidle, S. (2002) Crystal structure of parallel quadruplexes from human telomeric DNA, *Nature 417*, 876−880.
11. Williamson, J. R., Raghuraman, M. K., and Cech, T. R. (1989) Monovalent cation induced structure of telomeric DNA: The G-quartet model, *Cell 59*, 871−880.
12. Sen, D., and Gilbert, W. (1990) A sodium-potassium switch in the formation of 4-stranded G4-DNA, *Nature 344*, 410−414.
13. Sen, D., and Gilbert, W. (1992) Guanine quartet structures, *Methods Enzymol. 211*, 191−199.
14. Sen, D., and Gilbert, W. (1988) Formation of parallel four-stranded complexes by guanine rich motifs in DNA and its implications for meiosis, *Nature 344*, 410−414.
15. Simonsson, T., Pecinka, P., and Kubista, M. (1998) DNA tetraplex formation in the control regions of c-myc, *Nucleic Acids Res. 26*, 1167−1172.
16. Rangan, A., Fedoroff, O. Y., and Hurley, L. H. (2001) Induction of duplex to G-quadruplex transition in the c-myc promoter region by a small molecule, *J. Biol. Chem. 276*, 4640−4646.
17. Siddiqui-Jain, A., Grand, C. L., Bearss, D. J., and Hurley, L. H. (2002) Direct evidence for a G-quadruplex in a promoter region and its targeting with a small molecule to repress c-MYC transcription, *Proc. Natl. Acad. Sci. U.S.A. 99*, 11593−11598.
18. Ambrus, A., Chen, D., Dai, J. X., Jones, R. A., and Yang, D. Z. (2005) Solution structure of the biologically relevant G-quadruplex element in the human c-MYC promoter. Implications for G-quadruplex stabilization, *Biochemistry 44*, 2048−2058.
19. Cogoi, S., and Xodo, L. E. (2006) G-Quadruplex formation within the promoter of the K-ras proto-oncogene and its effect on transcription, *Nucleic Acids Res. 34*, 2536−3549.
20. Dai, J. X., Dexheimer, T. S., Chen, D., Carver, M., Ambrus, A., Jones, R. A., and Yang, D. Z. (2006) An intramolecular G-quadruplex structure with mixed parallel/antiparallel G-strands formed in the human bcl-2 promoter region in solution, *J. Am. Chem. Soc. 128*, 1096−1098.
21. Dexheimer, T. S., Sun, D., and Hurley, L. H. (2006) Deconvoluting the structural and drug-recognition complexity of the G-quadruplex-forming region upstream of the bcl-2 P1 promoter, *J. Am. Chem. Soc. 128*, 5404−5415.
22. Rankin, S., Reszka, A P., Huppert, J., Zloh, M., Parkinson, G. N., Todd, A. K., Ladame, S., Balasubramanian, S., and Neidle, S. (2005) Putative DNA quadruplex formation within the human c-kit oncogene, *J. Am. Chem. Soc. 127*, 10584−10589.
23. Sun, Y., Guo, K. X., Rusche, J. J., and Hurley, L. H. (2005) Facilitation of a structural transition in the polypurine/polypyrimidine tract within the proximal promoter region of the human VEGF gene by the presence of potassium and G-quadruplex-interactive agents, *Nucleic Acids Res. 33*, 6070−6080.
24. De Armond, R., Wood, S., Sun, D. Y., Hurley, L. H., and Ebbinghaus, S. W. (2005) Evidence for the presence of a guanine quadruplex forming region within a polypurine tract of the hypoxia inducible factor 1α promoter, *Biochemistry 44*, 16341−16350.
25. Fry, M., and Loeb, M. A. (1994) The fragile-X syndrome $d(CGG)_n$ nucleotide repeats form a stable tetrahelical structure, *Proc. Natl. Acad. Sci. U.S.A. 91*, 4950−4954.
26. Matsugami, A., Okuizumi, T., Uesugi, S., and Katahira, M. (2003) Intramolecular higher order packing of parallel quadruplexes comprising a G:G:G:G tetrad and a G(:A):G(:A):G(:A):G heptad of GGA triplet repeat DNA, *J. Biol. Chem. 278*, 28147−28153.
27. Murchie, A. I., and Lilley, D. M. J. (1992) Retinoblastoma susceptibility genes contain 5′ sequences with a high propensity to form guanine-tetrad structures, *Nucleic Acids Res. 20*, 49−53.
28. Howell, R. M., Woodford, K. J., Weitzmann, M. N., and Usdin, K. (1996) The chicken β-globin gene promoter forms a novel "cinched" tetrahelical structure, *J. Biol. Chem. 271*, 5208−5214.

29. Lew, A., Rutter, W. J., and Kennedy, G. C. (2000) Unusual DNA structure of the diabetes susceptibility locus IDDM2 and its effect on transcription by the insulin promoter factor Pur-1/MAZ, *Proc. Natl. Acad. Sci. U.S.A. 97*, 12508−12512.
30. Yafe, A., Etzioni, S., Weisman-Shomer, P., and Fry, M. (2005) Formation and properties of hairpin and tetraplex structures of guanine-rich regulatory sequences of muscle-specific genes, *Nucleic Acids Res. 33*, 2887−2990.
31. Todd, A. K., Johnston, M., and Neidle, S. (2005) Highly prevalent putative quadruplex sequence motifs in human DNA, *Nucleic Acids Res. 33*, 2901−2907.
32. Huppert, J. L., and Balasubramanian, S. (2005) Prevalence of quadruplexes in the human genome, *Nucleic Acids Res. 33*, 2908−2916.
33. Huppert, J. L.; and Balasubramanian, S. (2007) G-quadruplexes in promoters throughout the human genome. *Nucleic Acids Res. 35*, 406−413.
34. Li, J., Correia, J. J., Wang, L., Trent, J. O., and Chaires, J. B. (2005) Not so crystal clear: The structure of the human telomere G-quadruplex in solution differs from that present in a crystal, *Nucleic Acids Res. 33*, 4649−4659.
35. Phan, A. T., and Patel, D. J. (2003) Two repeat human telomeric d(TAGGGTTAGGGT) sequence forms interconverting parallel and antiparallel G-quadruplexes in solution: Distinct topologies, thermodynamic properties and folding/unfolding kinetics, *J. Am. Chem. Soc. 125*, 15021−15027.
36. Rujan, I. N., Meleney, J. C., and Bolton, P. H. (2005) Vertebrate telomere repeat DNAs favour external propeller quadruplex structures in the presence of high concentrations of potassium, *Nucleic Acids Res. 33*, 2022−2031.
37. Ambrus, A., Chen, D., Dai, J. X., Bialis, T., Jones, R. A., and Yang, D. Z. (2006) Human telomeric sequence forms a hybrid-type intramolecular G-quadruplex structure with mixed parallel/antiparallel strands in potassium solution, *Nucleic Acids Res. 34*, 2723−2735.
38. Luu, K. N., Phan, A. T., Kuryavyi, V., Lacroix, L., and Patel, D. J. (2006) Structure of the human telomere in K^+ solution: An intramolecular (3+1) G-quadruplex, *J. Am. Chem. Soc. 128*, 9963−9970.
39. Xu, Y., Noguchi, Y., and Sugiyama, H. (2006) The new models of the human telomere d[AGGG(TTAGGG)$_3$] in solution, *Bioorg. Med. Chem. 14*, 5584−5591.
40. Risitano, A., and Fox, K. R. (2003) Stability of intramolecular DNA quadruplexes: Comparison with DNA duplexes, *Biochemistry 42*, 6507−6513.
41. Hazel, P., Huppert, J., Balasubramanian, S., and Neidle, S. (2004) Loop-length-dependent folding of G-quadruplexes, *J. Am. Chem. Soc. 126*, 16405−16415.
42. Risitano, A., and Fox, K. R. (2004) Influence of loop size on the stability of intramolecular DNA quadruplexes, *Nucleic Acids Res. 32*, 2598−2606.
43. Smirnov, I., and Shafer, R. H. (2000) Effect of loop sequence and size on DNA aptamer stability, *Biochemistry 39*, 1462−1468.
44. Lu, M., Guo, Q., and Kallenbach, N. R. (1992) Structure and stability of sodium and potassium complexes of dT_4G_4 and dT_4G_4T, *Biochemistry 31*, 2455−2459.
45. Guo, Q., Lu, M., and Kallenbach, N. R. (1993) Effect of thymine tract length on the structure and stability of model telomeric sequences, *Biochemistry 32*, 3596−3603.
46. Merkina, E. E., and Fox, K. R. (2005) Kinetic stability of intermolecular DNA quadruplexes, *Biophys. J. 89*, 365−373.
47. Phan, A. T., Modi, Y. S., and Patel, D. J. (2004) Two-repeat *Tetrahymena* telomeric d(TGGGGTTGGGGT) sequence interconverts between asymmetric dimeric G-quadruplexes in solution, *J. Mol. Biol. 338*, 93−102.
48. Wang, Y., and Patel, D. J. (1994) Solution structure of the *Tetrahymena* telomeric repeat $d(T_2G_4)_4$ G-tetraplex, *Structure 2*, 1141−1156.
49. Darby, R. A. J., Sollogoub, M., McKeen, C., Brown, L., Risitano, A., Brown, N., Barton, C., Brown, T., and Fox, K. R. (2002) High throughput measurement of duplex, triplex and quadruplex melting curves using molecular beacons and a LightCycler, *Nucleic Acids Res. 30*, e39.
50. Balagurumoorthy, P., Brahmachari, S. K., Mohanty, D., Bansal, M., and Sasisekharan, V. (1992) Hairpin and parallel quartet structures for telomeric sequences, *Nucleic Acids Res. 20*, 4061−4067.
51. Balagurumoorthy, P., and Brahmachari, S. K. (1994) Structure and stability of human telomeric sequence, *J. Biol. Chem. 269*, 21858−21869.
52. Lu, M., Guo, Q., and Kallenbach, N. R. (1993) Thermodynamics of G-tetraplex formation by telomeric DNAs, *Biochemistry 32*, 598−601.
53. Mergny, J. L., and Lacroix, L. (2003) Analysis of thermal melting curves, *Oligonucleotides 13*, 515−537.
54. Jing, N., Rando, R. F., Pommier, Y., and Hogan, M. E. (1997) Ion selective folding of loop domains in a potent anti-HIV oligonucleotide, *Biochemistry 36*, 12498−12505.
55. Cantor, C. R., and Schimmel, P. R. (1980) *Biophysical Chemistry*, W. H. Freedman and Co., New York.
56. Mergny, J.-L., and Maurizot, J.-C. (2001) Fluorescence resonance energy transfer as a probe for G-quartet formation by a telomeric repeat, *ChemBioChem 2*, 124−132.
57. Jing, N., and Hogan, M. E. (1998) Structure-activity of tetrad-forming oligonucleotides as a potential anti-HIV therapeutic drug, *J. Biol. Chem. 273*, 34992−34999.
58. Jing, N., Marchand, C., Liu, J., Mitra, R., Hogan, M. E., and Pommier, Y. (2000) Mechanism of inhibition of HIV-1 integrase by G-tetrad forming oligonucleotides in vitro, *J. Biol. Chem. 275*, 21460−21467.
59. Phan, A. T., Kuryavyi, V., Ma, J. B., Faure, A., Andreola, M. L., and Patel, D. J. (2005) An interlocked dimeric parallel-stranded DNA quadruplex: A potent inhibitor of HIV-1 integrase, *Proc. Natl. Acad. Sci. U.S.A. 102*, 634−639.
60. Esposito, V., Randazzo, A., Piccialli, G., Petraccone, L., Giancola, C., and Mayol, L. (2004) Effects of an 8-bromodeoxyguanosine incorporation on the parallel quadruplex structure [d(TGGGT)]$_4$, *Org. Biomol. Chem. 2*, 313−318.
61. Đapić, V., Abdomerović, V., Marrington, R., Peberdy, J., Rodger, A., Trent, J. O., and Bates, P. J. (2003) Biophysical and biological properties of quadruplex oligodeoxyribonucleotides, *Nucleic Acids Res. 31*, 2097−2107.

BI062118J